Solar Energy Materials & Solar Cells 95 (2011) 2443–2447

Contents lists available at ScienceDirect

Solar Energy Materials & Solar Cells

journal homepage: www.elsevier.com/locate/solmat

The effect of a concentration graded cathode for organic solar cells

Ji Hye Jeon [a], Hang Ken Lee [a], Dong Hwan Wang [a], Soon Mi Park [b], Jeong Won Kim [b], Kyung Joong Kim [b], Jong Hyeok Park [c,*], O Ok Park [a,*]

[a] Department of Chemical and Biomolecular Engineering (BK21 Graduate Program), Korea Advanced Institute of Science and Technology, 291 Deahak-ro, Yuseong-gu, Daejeon 305-701, Republic of Korea
[b] Korea Research Institute of Standards and Science (KRISS), Yuseong, Daejeon 305-600, Republic of Korea
[c] Department of Chemical Engineering, Sungkyunkwan University, Suwon 440-746, Republic of Korea

ARTICLE INFO

Article history:
Received 31 January 2011
Received in revised form
12 April 2011
Accepted 17 April 2011
Available online 4 May 2011

Keywords:
Organic photovoltaic
Li:Al alloy
Aluminum–carbon complex
Concentration graded cathode

ABSTRACT

We present the effects of a concentration graded Li:Al cathode when it is made by one-step evaporation method using single alloy sources on the performance of organic solar cells. The concentration profile of the Li:Al cathode and related interface energy levels were investigated by means of secondary ion mass spectroscopy and ultraviolet photoelectron spectroscopy, in comparison with those of a common Al cathode. The results indicate that interfacial lithium accumulation introduces a cascade decrease of the work function (WF) of the cathode. The WF graded cathode applied to bulk heterojunction solar cells resulted in increased short circuit current and power conversion efficiency. Furthermore, the Li:Al cathode avoids the formation of interface Al–C complex, which may cause disruption of electron transport.

1. Introduction

Solar energy is one of the promising renewable energy sources. Among various solar energy technologies, organic solar cells (OSCs) have many advantages, including low cost, large area, and ease of processing [1–8]. However, the low efficiency of OSCs remains a challenging problem for their commercialization [9,10]. In efforts to enhance the efficiency of OSCs, many researchers have studied charge collection methods that involve controlling the interface between the active layer and electrode [11–17]. Several OSCs with an interlayer, such as 2,2′-azobis(2-methylpropionitrile), titanium oxide, polyethylene oxide, and molybdenum oxide, showed enhanced performance [4,12–15]. The interlayer serves to protect the organic layer during metal deposition and also facilitates charge collection [16,17]. Other researcher groups introduced alkaline layers such as lithium fluoride (LiF), sodium fluoride, and potassium fluoride between the active layer and cathode.[14–17] Insertion of a thin alkaline-fluoride layer (~1 nm) increases the open-circuit voltage (V_{oc}) of the OSC, because the interlayer promotes strong dipole formation [16,17]. Accordingly, many researchers have attempted to increase efficiency through insertion of different types of interlayers. However, the inserted interlayer requires another vacuum deposition process, and the controlling of an extremely thin layer (under 1–10 nm) during vacuum deposition could be a very difficult task.

In this paper, we have prepared an Al cathode incorporating concentration-graded Li metal for application in OSCs. Using a Li:Al single alloy source for cathode formation, we successfully fabricated the concentration graded cathode by an one-step process. Because the Li metal evaporates faster at a lower temperature than Al, it is anticipated that the concentration of Li metal will be higher at the surface of underlying active layer after overall thermal evaporation. The Li accumulation at the interface effectively avoids the penetration of carbon (active material) into the cathode so that it would reduce the formation of Al–C complex, which may disrupt electron transport. Such interfacial Li atoms also generate interface dipole that helps electron collection to the cathode.

2. Experimental

2.1. Film and device fabrication

In this experiment, bulk-heterojunction photovoltaic cells with a structure of indium tin oxide (ITO)/poly(3,4-ethylene dioxythiophene:poly(styrene sulfonate)(PEDOT:PSS)/poly(3-hexylthiophene) (P3HT)), and [6,6]-phenyl-C-61-buytyric acid methyl ester (PCBM) blends (P3HT:PCBM)/Li:Al were fabricated. The device structure of OSCs using this Li:Al cathode is schematically illustrated in Fig. 1(a). To prepare the devices, ITO glass was cleaned and then exposed to oxygen plasma for 10 min prior to use. A buffer layer of PEDOT:PSS (Clavios P) was then spin-coated to a thickness of ~40 nm and

* Corresponding authors.
E-mail addresses: lutts@skku.edu (J.H. Park), ookpark@kaist.ac.kr (OO. Park).

0927-0248/$ - see front matter © 2011 Elsevier B.V. All rights reserved.
doi:10.1016/j.solmat.2011.04.026

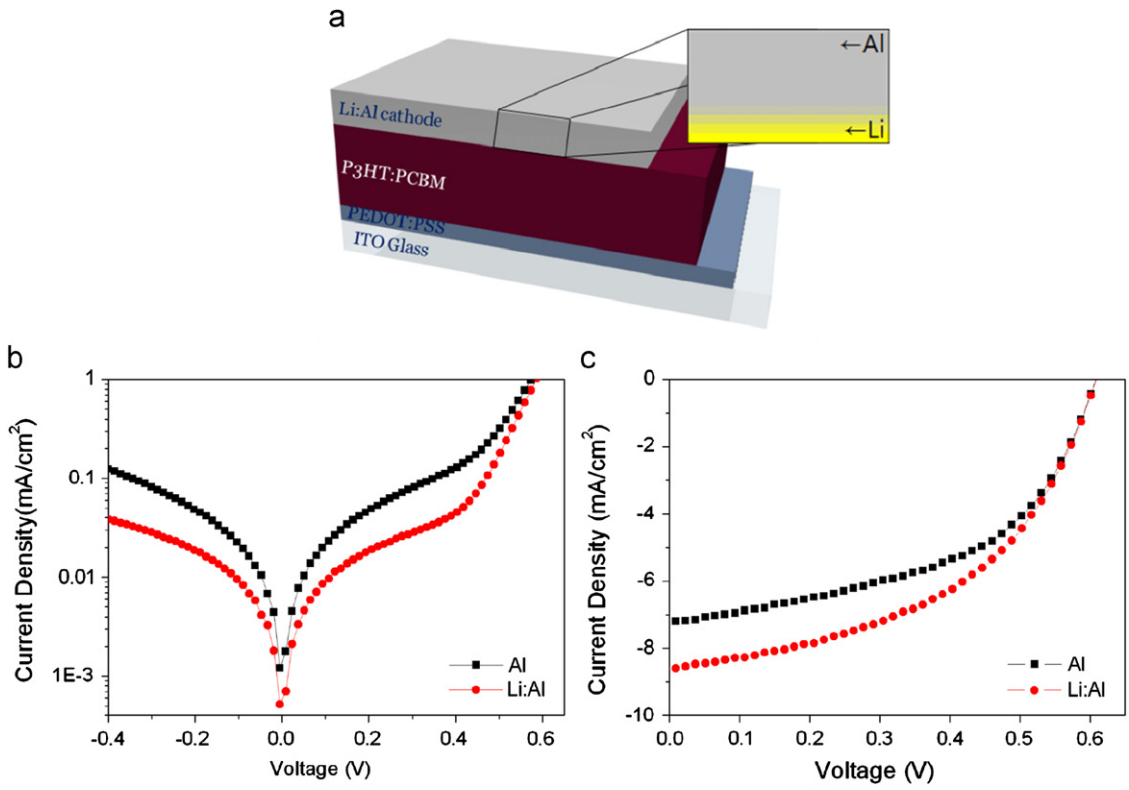

Fig. 1. (a) Device structure of organic solar cells on Li:Al alloy cathode. Dark (b) and illumination (c) *J–V* curves of the photovoltaic cells with aluminum cathode (■) and Li:Al cathode (●).

baked at 200 °C for 5 min. An active layer composed of P3HT (Rieke Met. Inc.) and PCBM (Nano-C) (1:0.6 in weight ratio) was spin-coated from chlorobenzene with 220 ± 5 nm thin films. The metal electrode is comprised of Li:Al (Kurt J. lesker Li 0.3 wt%) or Al (Cerac inc. 99.999%), and was thermally deposited using a thermal evaporator to a thickness of 150 nm. Both processes were performed under the vacuum of 3×10^{-6} Torr. After the deposition, thermal annealing of the samples was performed at 150 °C for 30 min. The defined active area was 4–5 mm^2, as determined using digital microscope.

2.2. Measurement

The current–voltage characteristics (*J–V*) of photovoltaic cells in the dark and under a simulated AM 1.5 white light illumination were measured with a Hewlett-Packard 4155A semiconductor parameter analyzer (Yokohama Hewlett-Packard, Tokyo). The voltage scan rate was a 20 mV/s from positive potential to negative potential. The AM 1.5 white light was produced from a solar simulator based on a filtered Xe lamp (Oriel, 91193) and its intensity was adjusted with a Si reference cell (Fraunhofer ISE, certificate no. C-ISE269) for 1 sunlight intensity of 100 mW/cm^2. All the photovoltaic properties were evaluated in ambient air at room temperature (from 20 to 22 °C). For ultraviolet photoelectron spectroscopy (UPS) measurements, active layers were spin cast on precleaned ITO substrates and then the samples were also kept in a high vacuum chamber overnight to remove residual solvent. We deposited Al and Li:Al thin films by water-cooled Knudsen cells in an ultra-high vacuum (UHV) system under a pressure of about 2.4×10^{-8} Torr. The typical deposition rate was 4 Å/min, monitored by a quartz crystal microbalance. Samples were subsequently transferred to an analysis chamber to investigate the interface electronic structures before and after each film deposition without exposure to air. UPS measurements were performed in UHV using a hemispherical electron energy analyzer (VG-Scienta SES-100) and a He I ultraviolet source ($\hbar\omega = 21.2$ eV) without a monochromator. UPS spectra were obtained with a sample bias of -10 and -5 V for secondary electron cutoff and highest occupied molecular orbital (HOMO) regions, respectively. Total energy resolution of the UPS spectra was less than 0.1 eV.

3. Results and discussion

Fig. 1 shows the dark (b) and illuminated (c) the *J–V* curves of OSCs prepared with Li:Al and Al cathodes, respectively. It can be seen from Fig. 1(b) that the dark current of the solar cells was lowered by about five times upon replacing Al with Li:Al cathode. The curves of illuminated *J–V* for the two devices using different cathodes are shown in Fig. 1(c). To ensure reproducibility, we fabricated five cells for each case (Table 1) and all the parameters are represented as mean values. The device with the Al cathode has a short circuit current (J_{sc}) of 7.42 ± 0.64 (mA/cm^2), open-circuit voltage (V_{oc}) of 0.6 ± 0.01 (V), calculated fill factor (FF) of 0.52 ± 0.01, and power conversion efficiency (PCE) of 2.31 ± 0.19 (%). The device with the Li:Al cathode has a J_{sc} of 8.33 ± 0.43 (mA/cm^2), of 0.62 ± 0.01 (V), FF of 0.49 ± 0.01, and PCE of 2.51 ± 0.11 (%).

From above, it turns out that the cells made of Li–Al alloy for the cathode always had a higher J_{sc} (from 7.42 to 8.33 mA/cm^2), while the changes in V_{oc} were marginal. The insertion of a buffer layer such as LiF may increase V_{oc} reported in [16]. However, here for cells with Li:Al cathode, the increased photocurrent was observed to enhance the efficiency with marginal change in V_{oc}, a dominant factor for enhanced cell efficiency. This improvement might be attributed to work function (WF) engineering of the cathode and hindered formation of Al–C complex as suggested in [18].

To confirm the WF effect and Al–C complex formation of the Li:Al cathode in OSC devices, the interface between active layer

and cathode was analyzed using UPS and secondary ion mass spectrometry (SIMS). Fig. 2(a) and (c) shows the UPS spectra around the Fermi level when two different cathode materials with various film thicknesses were deposited on P3HT:PCBM, respectively. And the WF variation as a function of cathode film thickness was measured. Based on these measurements the energy diagram at the active layer and cathode interface referenced to Fermi level (E_F) was drawn as shown in Fig. 2(b) and (d).

Initial WFs of P3HT:PCBM layers shown in Fig. 2(b) and (d) were 4.22 and 4.12 eV, respectively. These values were directly obtained from UPS measurements. The HOMO positions of the layers in Fig. 2(a) and (c) are 0.45 and 0.55 eV referenced to Fermi level [19]. The ionization energies of both the P3HT:PCBM layers are 4.67 eV. Upon the deposition of first 2 Å of Al, the WF was lowered to 3.94 eV. However, when 2 Å of Li:Al was deposited, the WF value was 3.53 eV. Their corresponding HOMO positions are lowered to 0.65 and 0.8 eV, respectively. The direction of these band bending is the same as that of WF lowering, but the difference in their

Table 1
The cell performances of organic solar cells with different cathodes (Al, Li:Al).

V_{oc} (V)		J_{sc} (mA/cm^2)		FF		PCE (%)	
Li:Al	**Al**	**Li:Al**	**Al**	**Li:Al**	**Al**	**Li:Al**	**Al**
0.6123	0.5819	8.5543	8.5485	0.5104	0.5299	2.6733	2.636
0.6213	0.6086	7.7725	6.9469	0.4975	0.525	2.4024	2.2199
0.6254	0.6144	7.9554	7.2252	0.4842	0.5162	2.4094	2.2915
0.6088	0.6082	8.7079	7.1474	0.4807	0.5049	2.5483	2.1948
0.6151	0.6066	8.6557	7.2139	0.4748	0.505	2.5279	2.2098

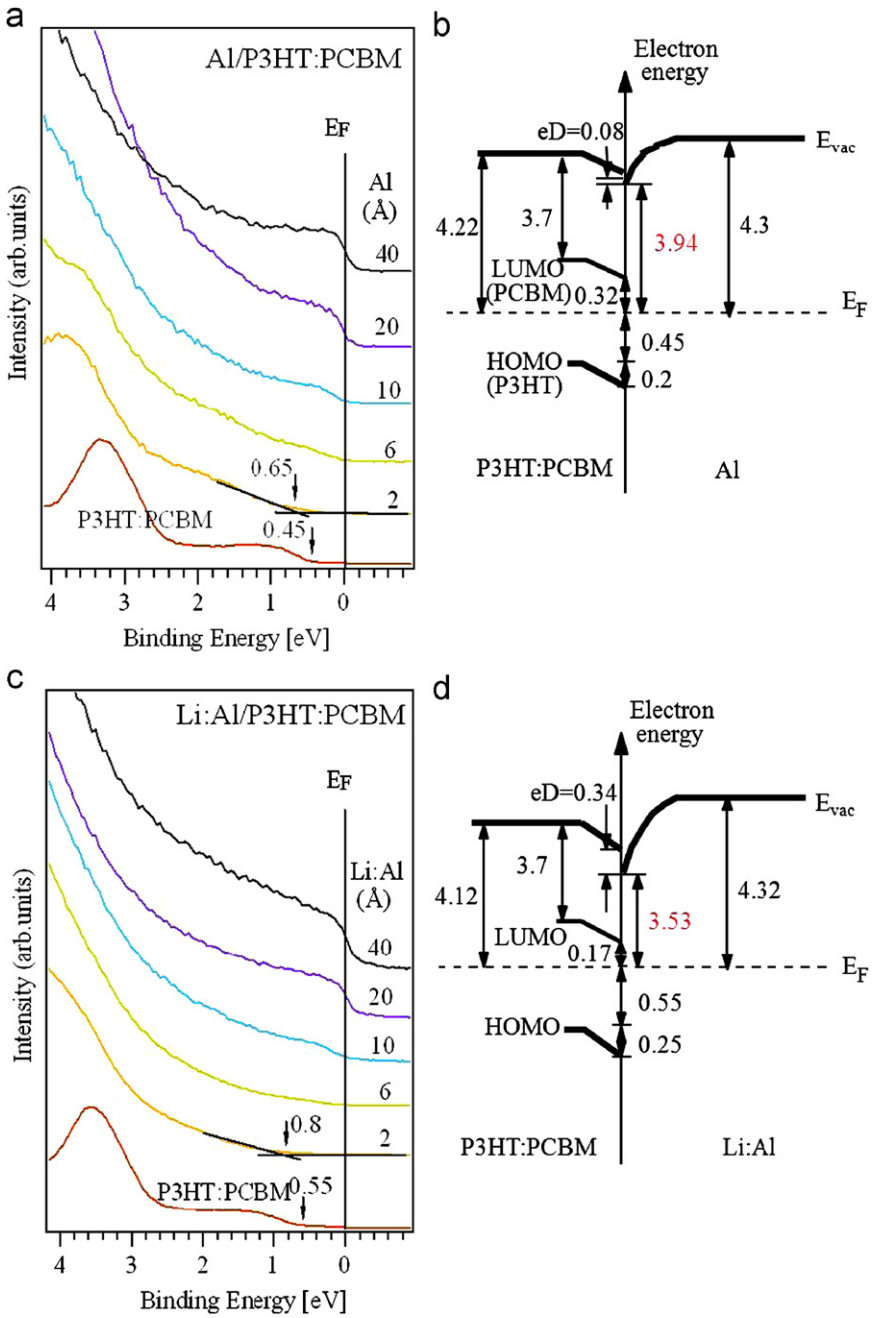

Fig. 2. Hel UPS spectra of deposition of Al (a) and Li:Al (c) with thickness of 2–40 Å on P3HT:PCBM coated glass. Energy level diagram for P3HT:PCBM/Al (b) and Li:Al (d) interface constructed from data obtained by UPS.

magnitudes (0.25–0.2=0.05 eV) is marginal when it compared with WF difference between Al (3.94 eV) and Li:Al (3.53 eV). When the cathode thickness exceeds 6 Å, the HOMO position of the active layer can no longer be identified, but metallic Fermi edge becomes distinct.

The electrons separated from the excitons in the active layer should be extracted at the interface between PCBM and the cathode electrode [2]. Since the lowest unoccupied molecular orbital (LUMO) of PCBM is located at 3.7 eV below vacuum level (E_{vac}), the band gap between the HOMO of P3HT and the LUMO of PCBM is estimated to be 0.97 eV. As mentioned above, the bending of their molecular energy level in contact with either Al or Li:Al does not give a big difference (0.20 eV for Al vs. 0.25 eV for Li:Al). However, the WF lowering after Li:Al deposition is more dominant compared to Al deposition (3.94 eV for Al vs. 3.53 eV for Li:Al), resulting the formation of a strong interface dipole (eD) (potential difference of vacuum level at the interface=band bending+dipole moment) at the P3HT:PCBM/Li:Al (eD=0.08 eV for Al vs. 0.34 eV for Li:Al). As a result, the PCBM in contact with Li:Al cathode feels lower barrier for electron injection to cathode (3.93–0.32=3.61 eV for Al vs. 3.53–0.17=3.36 eV for Li:Al). It is easily understood that the incorporation of Li lowers the work function of the metal cathode [20], since the WF of bulk Li (2.9 eV) is lower than that of Al (4.3 eV) [17]. As the Al thickness increases, the WF increases to reach 4.3 eV as expected. The Li:Al also shows similar behavior since most Li atoms are deposited only at the very first stage. From above results, it can be assumed that the concentration of Li should be higher at the interface between the active layer and cathode and this would cause higher electron collection efficiency.

Depth distributions of carbon and lithium in the cathode layer were analyzed by dynamic SIMS as shown in Fig. 3. Thin films of Al (40 nm), Li:Al (40 nm), and LiF/Al (0.6/39.4 nm) cathodes were deposited on the active layers to investigate both C and Li profiles mainly near the interface. The flat depth profiles of aluminum are omitted here because of abundant amount of Al in the first place. Li was detected about 10 nm range (30–40 nm depth) on the active layer in the case of the Li:Al cathode. This provides clear evidence of Li metal doping in Al and indicates that Li evaporates more rapidly than Al because Li and Al have different thermal properties (Li: melting point=453.7 K, boiling point=1615 K, Al: melting point=931.25 K, boiling point=2793 K) [21,22].

Carbon was also detected within the metal electrode of 40 nm thickness as shown in Fig. 3. The distribution of carbon in the shallow depth means the interdiffusion of Al of the electrode and C of the active layer. However, the distribution of carbon was observed at much shallower depth in the pure Al than the Li:Al cathode. This indicates that lithium evaporated first and can protect the active layer from damage by penetration of the Al cathode material. A similar observation was also reported by Greczynski et al. [18]. They reported that a LiF interlayer can protect the active layer from Al–C complex formation. To compare the blocking effect of Li with LiF, 40 nm-thick LiF (0.6 nm)/Al (39.4 nm) based cathode was also prepared on the active layer. To obtain optimized cell performance, the thickness of LiF was controlled to have 0.6 nm. As can be seen in Fig. 3, the concentration profile of carbon was still observed more earlier than the Li:Al cathode. This represent that the Li:Al cathode is more effective to block the formation of Al–C complex due to the unwanted penetration of Al source into the active layer. The formation of Al–C complex disrupts π-conjugation along the backbone and interrupts efficient electron transport in polymer solar cells. This behavior can also contribute to an increase of the J_{sc} value in bulk heterojunction cells.

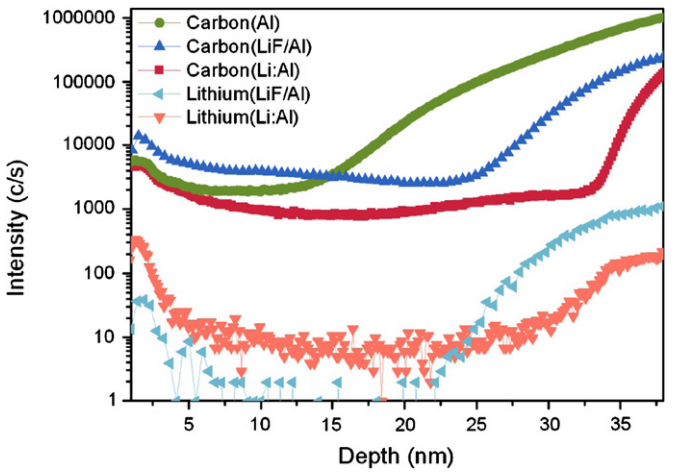

Fig. 3. SIMS depth profiles of Li and C in the organic solar cell devices with different cathodes (Al, Li:Al, and LiF/Al).

4. Conclusions

We fabricated organic photovoltaic cells with a Li:Al concentration graded cathode using a simple one-step thermal evaporation method. Concentration graded Li metal, which evaporates before Al due to its lower melting point, from the top of active layer to the Al cathode may induce cascade WF lowering from the LUMO energy level to the WF of Al. The cascade lowered WF of the Li:Al cathode lowers the energy barrier for electron transport from the active layer to the cathode and thereupon affects the charge collection efficiency. Furthermore, the Li:Al cathode showed reduced formation of Al–C complex, which disrupts electron transport. This results in improved J_{sc} and overall photovoltaic efficiency.

Acknowledgment

This research was supported by a WCU Grant (R32-2008-000-10142-0) and ERC Program (R11-2007-045-01002-0(2009)) from MEST. J. H. Park acknowledges Research Programs through the NRF Grant funded by MEST (2011-0006268 and Future-based Technology Development Program (Nano Fields) (2010-0029321)).

References

[1] S. Gunes, H. Neugebauer, N.S. Sariciftci, Conjugated polymer-based organic solar cells, Chem. Rev. 107 (2007) 1324–1338.
[2] C.J. Brabec, N.S. Sariciftci, J.C. Hummelen, Plastic solar cells, Adv. Funct. Mater. 11 (2001) 15–26.
[3] B.C. Thompson, J.M.J. Frechet, Polymer–fullerene composite solar cells, Angew. Chem. Int. Ed. 47 (2008) 58–77.
[4] D.H. Wang, D.G. Choi, K.J. Lee, J.H. Jeong, S.H. Jeon, O.O. Park, J.H. Park, Effect of the ordered 2D-dot nano-patterned anode for polymer solar cells, Org. Electron. 11 (2010) 285–290.
[5] S.A. Gevorgyan, M. Jorgensen, F.C. Krebs, A setup for studying stability and degradation of polymer solar cells, Sol. Energy Mater. Sol. Cells 92 (2008) 736–745.
[6] M. Helgensen, R. Sondergaard, F.C. Krebs, Advanced materials and processes for polymer solar cell devices, J. Mater. Chem. 20 (2010) 36–60.
[7] T.T. Larsen-Olsen, E. Bundgaard, K.O. Sylvester-Hvid, F.C. Krebs, A solution process for inverted tandem solar cells, Org. Electron. 12 (2011) 364–371.
[8] R. Sondergaard, M. Helgesen, M. Jorgensen, F.C. Krebs, Fabrication of polymer solar cells using aqueous processing for all layers including the metal back electrode, Adv. Energy Mater. 1 (2011) 68–71.
[9] K. Norrman, N.B. Larsen, F.C. Krebs, Lifetimes of organic photovoltaics: combining chemical and physical characterization techniques to study degradation mechanisms, Sol. Energy Mater. Sol. Cells 90 (2006) 2793–2814.
[10] F.C. Krebs, K. Norrman, Analysis of the failure mechanism for a stable organic photovoltaic during 10000 h of testing, Prog. Photovolt.: Res. Appl. 15 (2007) 697–712.

[11] K. Norrman, F.C. Krebs, Lifetimes of organic photovoltaics: using TOF-SIMS and $^{18}O_2$ isotropic labeling to characterize chemical degradation mechanisms, Sol. Energy Mater. Sol. Cells 90 (2006) 213–227.

[12] H.K. Lee, J.H. Jeon, D.H. Wang, O.O. Park, J.K. Kim, S.H. Im, J.H. Park, Enhanced charge collection via nanoporous morphology in polymer solar cells, Appl. Phys. Lett. 96 (2010) 103–304.

[13] D.H. Wang, S.H. Im, H.K. Lee, J.H. Park, O.O. Park, Enhanced high-temperature long-term stability of polymer solar cells with a thermally stable TiO_x interlayer, J. Phys. Chem. C 113 (2009) 17268–17273.

[14] S.J. Yoon, J.H. Park, H.K. Lee, O.O. Park, Low vacuum process for polymer solar cells: effect of TiO_x interlayer, Appl. Phys. Lett. 92 (2008) 143504.

[15] F. Zhang, M. Ceder, O. Inganas, Enhancing the photovoltage of polymer solar cells by using a modified cathode, Adv. Mater. 19 (2007) 1835–1838.

[16] C.J. Brabec, S.E. Shaheen, C. Winder, N.S. Sariciftci, Effect of LiF/metal electrodes on the performance of plastic solar cells, Appl. Phys. Lett. 80 (2002) 1288–1290.

[17] E. Ahlswede, J. Hanisch, M. Powalla, Comparative study of the influence of LiF, NaF, and KF on the performance of polymer bulk heterojunction solar cells, Appl. Phys. Lett. 90 (2007) 163504.

[18] G. Greczynski, M. Fahlman, W.R. Salaneck, An experimental study of poly(9,9-dioctylfluorene)and its interfaces with Li, Al, and LiF, J. Chem. Phys. 113 (2000) 2407–2412.

[19] Z. Xu, L.-M. Chen, M.-H. Chen, G. Li, Y. Yang, Energy level alignment of poly(3-hexylthiophene): [6,6]-phenyl C_{61} butyric acid methyl ester bulk heterojunction, Appl. Phys. Lett. 95 (2009) 013301.

[20] H. Ishii, K. Sugiyama, E. Ito, K. Seki, Energy level alignment and interfacial electronic structures at organic/metal and organic/organic interfaces, Adv. Mater. 11 (1999) 605–625.

[21] Y.K. Kim, D.K. Choi, B.S. Moon, E.S. Oh, H.T. Lim, S.N. Kwon, C.S. Ha, Controllable work function of Li:Al alloy nanolayers for organic light-emitting devices, Adv. Eng. Mater. 7 (2005) 1023–1027.

[22] T. Wakimoto, Y. Fukuda, K. Nagayama, A. Yokoi, H. Nakada, M. Tsuchida, Organic EL cells using alkaline metal compounds as electron injection material, IEEE Trans. Electron. Devices 44 (1997) 1245–1248.